Active Damping of Rotating Positioning Platforms

T. Dehaeze [1,3]**, C. Collette** [1,2]
[1] Precision Mechatronics Laboratory
University of Liege, Belgium

[2] BEAMS Department
Free University of Brussels, Belgium

[3] European Synchrotron Radiation Facility
Grenoble, France e-mail: **thomas.dehaeze@esrf.fr**

Abstract
Abstract text to be done

1 Introduction

Controller Poles are shown by black crosses (✖). This paper has been published The Matlab code that was use to obtain the results are available in [1].

2 Dynamics of Rotating Positioning Platforms

2.1 Studied Rotating Positioning Platform

Consider the rotating X-Y stage of Figure 1.

- k: Actuator's Stiffness [N/m]
- m: Payload's mass [kg]
- $\Omega = \dot{\theta}$: rotation speed [rad/s]
- F_u, F_v
- d_u, d_v

2.2 Equation of Motion

The system has two degrees of freedom and is thus fully described by the generalized coordinates u and v (describing the position of the mass in the rotating frame).

Let's express the kinetic energy T and the potential energy V of the mass m (neglecting the rotational energy):

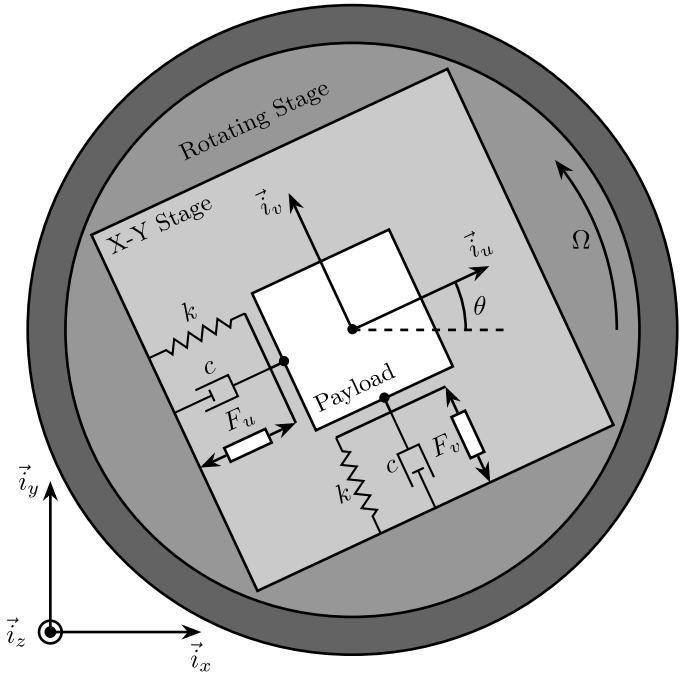

Figure 1: Schematic of the studied System

Dissipation function R Kinetic energy T Potential energy V

$$T = \frac{1}{2}m\left((\dot{u} - \Omega v)^2 + (\dot{v} + \Omega u)^2\right) \tag{1a}$$

$$R = \frac{1}{2}c\left(\dot{u}^2 + \dot{v}^2\right) \tag{1b}$$

$$V = \frac{1}{2}k\left(u^2 + v^2\right) \tag{1c}$$

The Lagrangian is the kinetic energy minus the potential energy:

$$L = T - V \tag{2}$$

From the Lagrange's equations of the second kind, the equation of motion is obtained ($q_1 = u$, $q_2 = v$).

$$\frac{d}{dt}\left(\frac{\partial L}{\partial \dot{q}_i}\right) + \frac{\partial D}{\partial \dot{q}_i} - \frac{\partial L}{\partial q_i} = Q_i \tag{3}$$

with Q_i is the generalized force associated with the generalized variable q_i ($Q_1 = F_u$ and $Q_2 = F_v$).

$$m\ddot{u} + c\dot{u} + (k - m\Omega)u = F_u + 2m\Omega\dot{v} \tag{4a}$$

$$m\ddot{v} + c\dot{v} + (k\underbrace{- m\Omega}_{\text{Centrif.}})v = F_v\underbrace{- 2m\Omega\dot{u}}_{\text{Coriolis}} \tag{4b}$$

- Coriolis Forces: coupling
- Centrifugal forces: negative stiffness

Without the coupling terms, each equation is the equation of a one degree of freedom mass-spring system with mass m and stiffness $k - m\dot{\theta}^2$. Thus, the term $-m\dot{\theta}^2$ acts like a negative stiffness (due to **centrifugal forces**).

2.3 Transfer Functions in the Laplace domain

$$u = \frac{ms^2 + cs + k - m\Omega^2}{\left(ms^2 + cs + k - m\Omega^2\right)^2 + \left(2m\Omega s\right)^2} F_u + \frac{2m\Omega s}{\left(ms^2 + cs + k - m\Omega^2\right)^2 + \left(2m\Omega s\right)^2} F_v \tag{5a}$$

$$v = \frac{-2m\Omega s}{\left(ms^2 + cs + k - m\Omega^2\right)^2 + \left(2m\Omega s\right)^2} F_u + \frac{ms^2 + cs + k - m\Omega^2}{\left(ms^2 + cs + k - m\Omega^2\right)^2 + \left(2m\Omega s\right)^2} F_v \tag{5b}$$

$$\begin{bmatrix} d_u \\ d_v \end{bmatrix} = \boldsymbol{G}_d \begin{bmatrix} F_u \\ F_v \end{bmatrix} \tag{6}$$

Where $\boldsymbol{G}_d$ is a 2×2 transfer function matrix.

$$\boldsymbol{G}_d = \frac{1}{k} \frac{1}{G_{dp}} \begin{bmatrix} G_{dz} & G_{dc} \\ -G_{dc} & G_{dz} \end{bmatrix} \tag{7}$$

With:

$$G_{dp} = \left(\frac{s^2}{{\omega_0}^2} + 2\xi\frac{s}{\omega_0} + 1 - \frac{\Omega^2}{{\omega_0}^2}\right)^2 + \left(2\frac{\Omega}{\omega_0}\frac{s}{\omega_0}\right)^2 \tag{8a}$$

$$G_{dz} = \frac{s^2}{{\omega_0}^2} + 2\xi\frac{s}{\omega_0} + 1 - \frac{\Omega^2}{{\omega_0}^2} \tag{8b}$$

$$G_{dc} = 2\frac{\Omega}{\omega_0}\frac{s}{\omega_0} \tag{8c}$$

- $\omega_0 = \sqrt{\frac{k}{m}}$: Natural frequency of the mass-spring system in $\mathrm{rad/s}$
- ξ damping ratio

2.4 Constant Rotational Speed

To simplify, let's consider a constant rotational speed $\dot{\theta} = \Omega$ and thus $\ddot{\theta} = 0$.

$$\begin{bmatrix} d_u \\ d_v \end{bmatrix} = \frac{1}{(ms^2 + (k - m{\omega_0}^2))^2 + (2m\omega_0 s)^2} \begin{bmatrix} ms^2 + (k - m{\omega_0}^2) & 2m\omega_0 s \\ -2m\omega_0 s & ms^2 + (k - m{\omega_0}^2) \end{bmatrix} \begin{bmatrix} F_u \\ F_v \end{bmatrix} \tag{9}$$

$$\begin{bmatrix} d_u \\ d_v \end{bmatrix} = \frac{\frac{1}{k}}{\left(\frac{s^2}{{\omega_0}^2} + (1 - \frac{\Omega^2}{{\omega_0}^2})\right)^2 + \left(2\frac{\Omega s}{{\omega_0}^2}\right)^2} \begin{bmatrix} \frac{s^2}{{\omega_0}^2} + 1 - \frac{\Omega^2}{{\omega_0}^2} & 2\frac{\Omega s}{{\omega_0}^2} \\ -2\frac{\Omega s}{{\omega_0}^2} & \frac{s^2}{{\omega_0}^2} + 1 - \frac{\Omega^2}{{\omega_0}^2} \end{bmatrix} \begin{bmatrix} F_u \\ F_v \end{bmatrix} \tag{10}$$

When the rotation speed is null, the coupling terms are equal to zero and the diagonal terms corresponds to one degree of freedom mass spring system.

$$\begin{bmatrix} d_u \\ d_v \end{bmatrix} = \frac{\frac{1}{k}}{\frac{s^2}{{\omega_0}^2} + 1} \begin{bmatrix} 1 & 0 \\ 0 & 1 \end{bmatrix} \begin{bmatrix} F_u \\ F_v \end{bmatrix} \tag{11}$$

When the rotation speed in not null, the resonance frequency is duplicated into two pairs of complex conjugate poles. As the rotation speed increases, one of the two resonant frequency goes to lower frequencies as the other one goes to higher frequencies (Figure 2).

The magnitude of the coupling terms are increasing with the rotation speed.

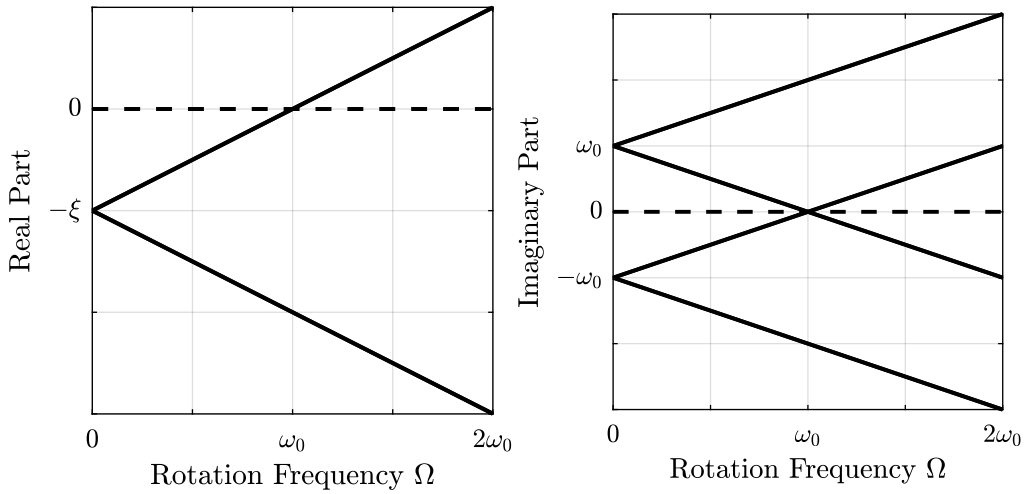

(a) Real Part

(b) Imaginary Part

Figure 2: Campbell Diagram : Evolution of the poles as a function of the rotational speed Ω

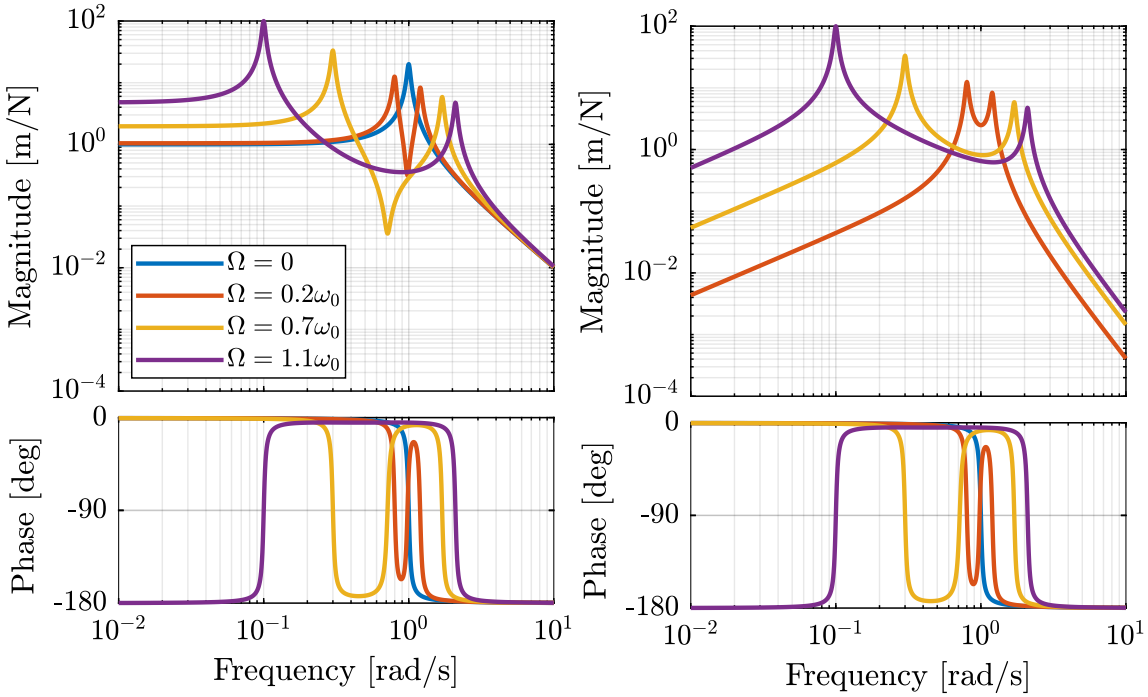

(a) Direct Terms d_u/F_u, d_v/F_v

(b) Coupling Terms d_v/F_u, d_u/F_v

Figure 3: Bode Plots for $\boldsymbol{G}_d$

3 Integral Force Feedback

3.1 Control Schematic

Force Sensors are added in series with the actuators as shown in Figure 4.

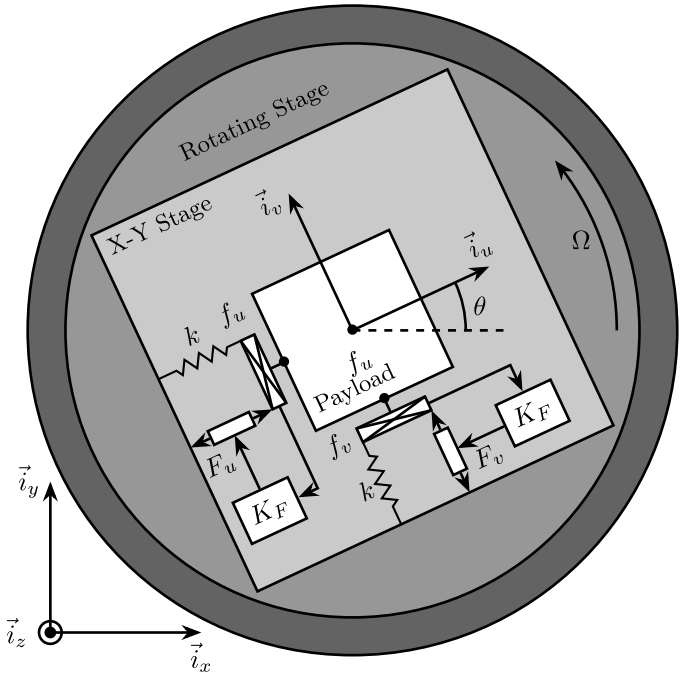

Figure 4: System with Force Sensors in Series with the Actuators. Decentralized Integral Force Feedback is used

3.2 Equations

The sensed forces are equal to:

$$\begin{bmatrix} f_u \\ f_v \end{bmatrix} = \begin{bmatrix} F_u \\ F_v \end{bmatrix} - (cs + k) \begin{bmatrix} d_u \\ d_v \end{bmatrix} \tag{12}$$

Which then gives:

$$\begin{bmatrix} f_u \\ f_v \end{bmatrix} = \boldsymbol{G}_f \begin{bmatrix} F_u \\ F_v \end{bmatrix} \tag{13}$$

$$\begin{bmatrix} f_u \\ f_v \end{bmatrix} = \frac{1}{G_{fp}} \begin{bmatrix} G_{fz} & -G_{fc} \\ G_{fc} & G_{fz} \end{bmatrix} \begin{bmatrix} F_u \\ F_v \end{bmatrix} \tag{14}$$

$$G_{fp} = \left(\frac{s^2}{{\omega_0}^2} + 2\xi \frac{s}{\omega_0} + 1 - \frac{\Omega^2}{{\omega_0}^2} \right)^2 + \left(2 \frac{\Omega}{\omega_0} \frac{s}{\omega_0} \right)^2 \tag{15}$$

$$G_{fz} = \left(\frac{s^2}{{\omega_0}^2} - \frac{\Omega^2}{{\omega_0}^2} \right) \left(\frac{s^2}{{\omega_0}^2} + 2\xi \frac{s}{\omega_0} + 1 - \frac{\Omega^2}{{\omega_0}^2} \right) + \left(2 \frac{\Omega}{\omega_0} \frac{s}{\omega_0} \right)^2 \tag{16}$$

$$G_{fc} = \left(2\xi \frac{s}{\omega_0} + 1 \right) \left(2 \frac{\Omega}{\omega_0} \frac{s}{\omega_0} \right) \tag{17}$$

3.3 Plant Dynamics

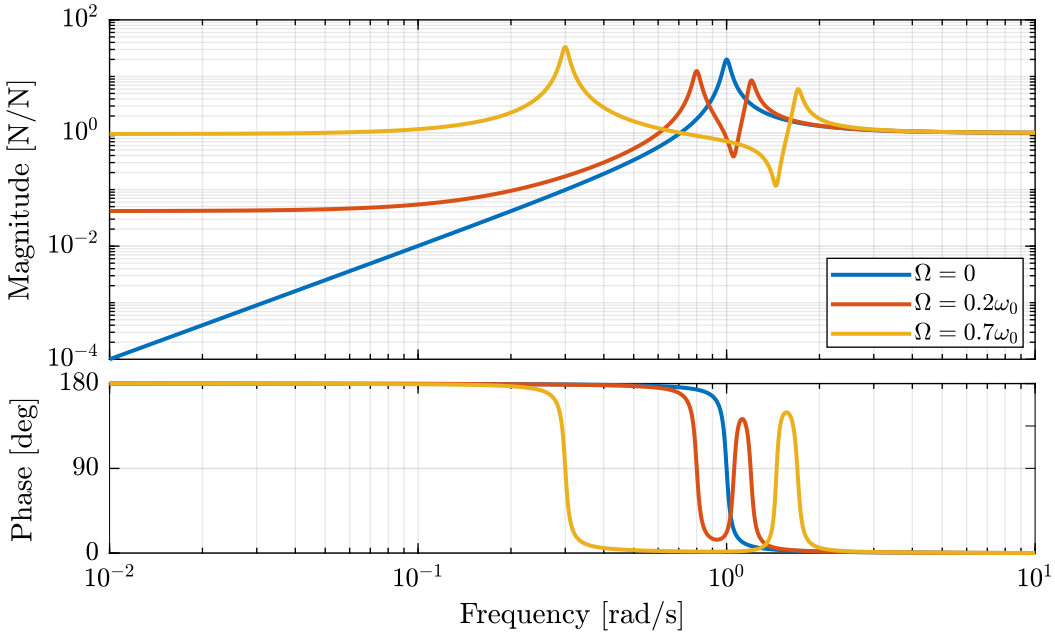

Figure 5: Bode plot of $\boldsymbol{G}_f$ for several rotational speeds Ω

3.4 Integral Force Feedback

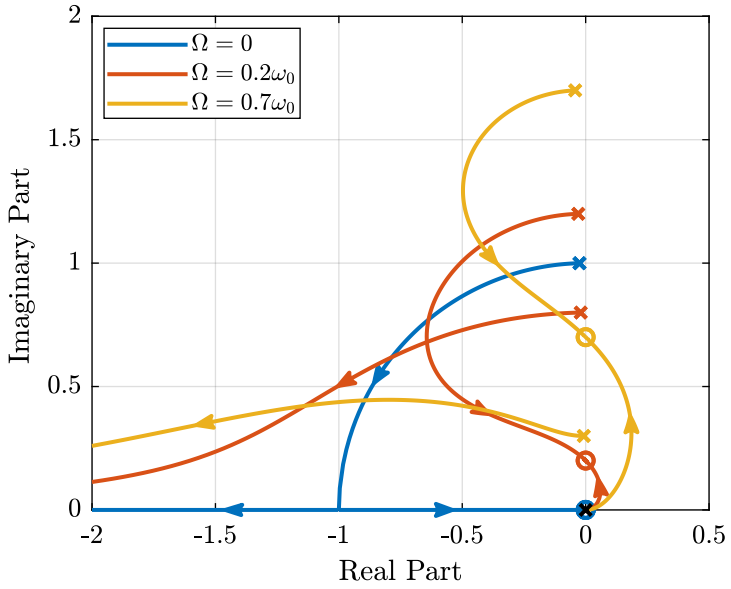

Figure 6: Root Locus for the Decentralized Integral Force Feedback

At low frequency, the gain is very large and thus no force is transmitted between the payload and the rotating stage. This means that at low frequency, the system is decoupled (the force sensor removed) and thus the system is unstable.

4 Integral Force Feedback with High Pass Filters

4.1 Modification of the Control Low

4.2 Feedback Analysis

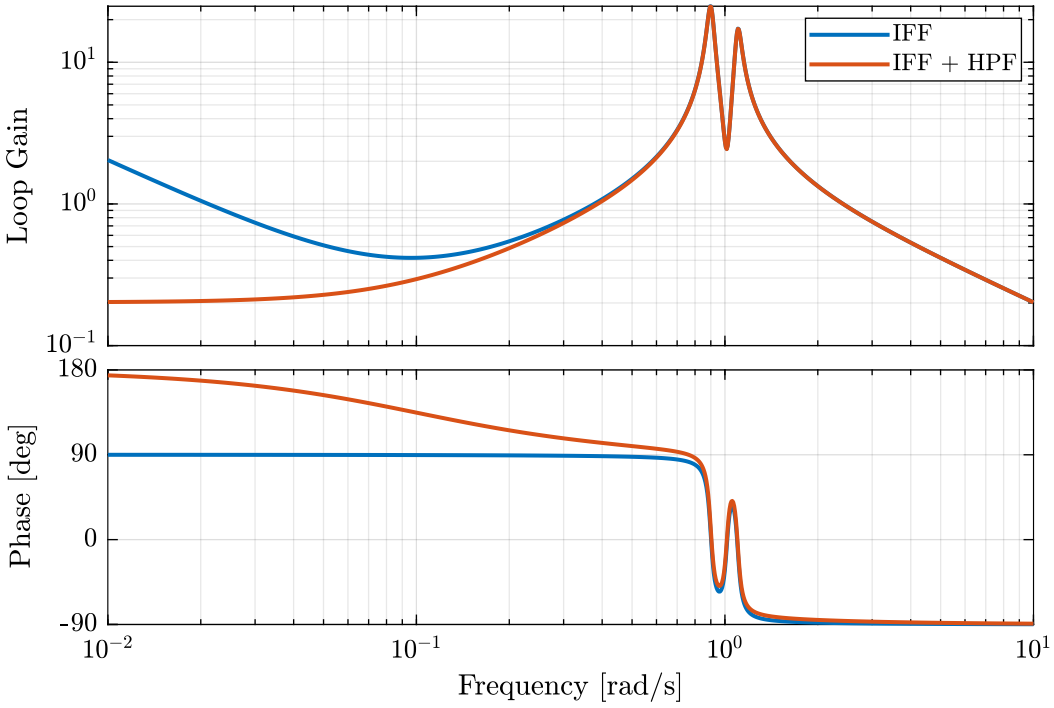

Figure 7: Bode Plot of the Loop Gain for IFF with and without the HPF

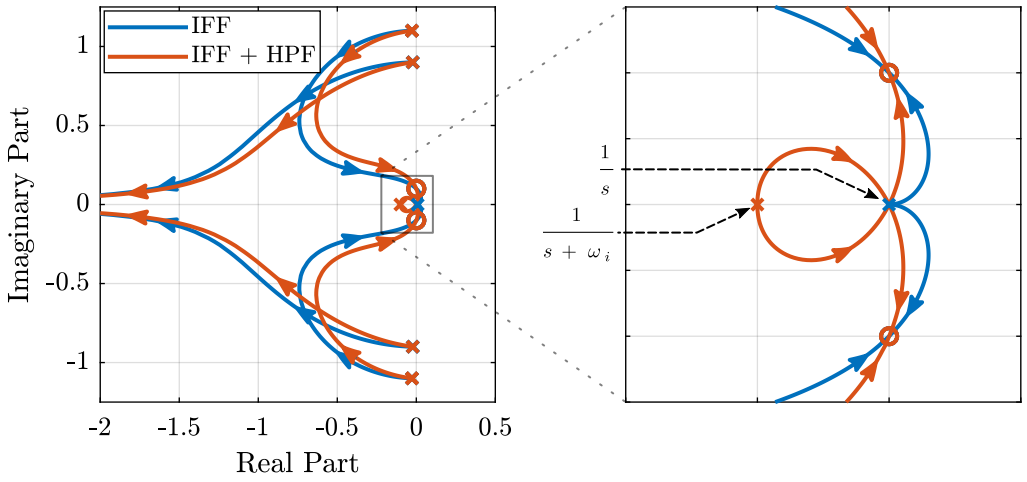

Figure 8: Root Locus for IFF with and without the HPF

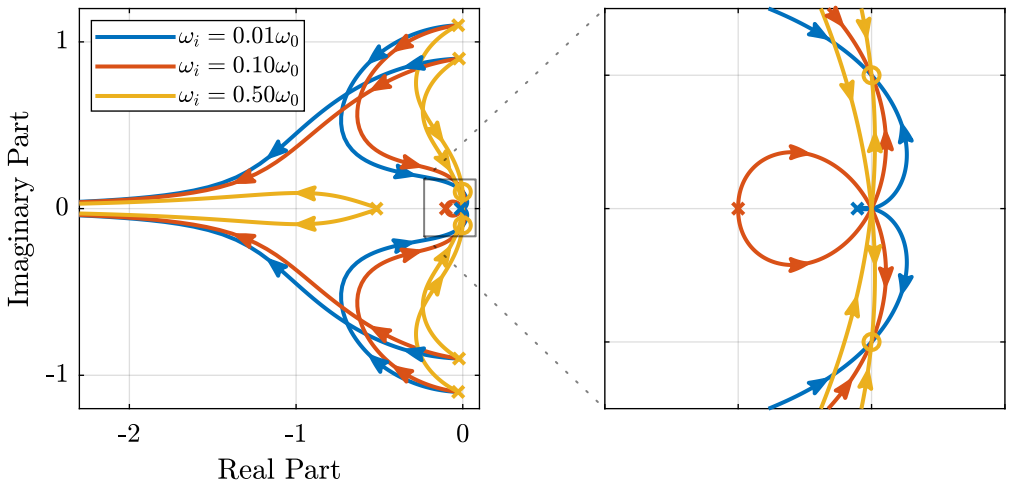

Figure 9: Root Locus for several HPF cut-off frequencies ω_i

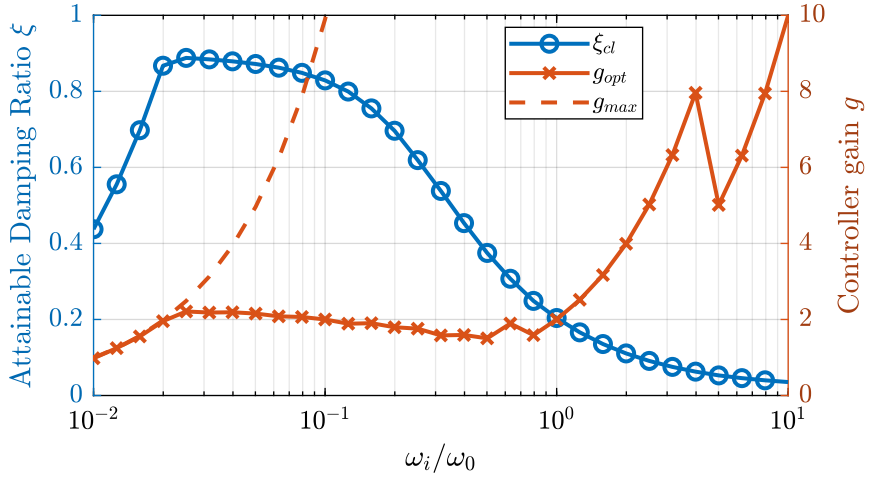

Figure 10: Attainable damping ratio ξ_{cl} as a function of the HPF cut-off frequency. Corresponding control gain g_{opt} and g_{max} are also shown

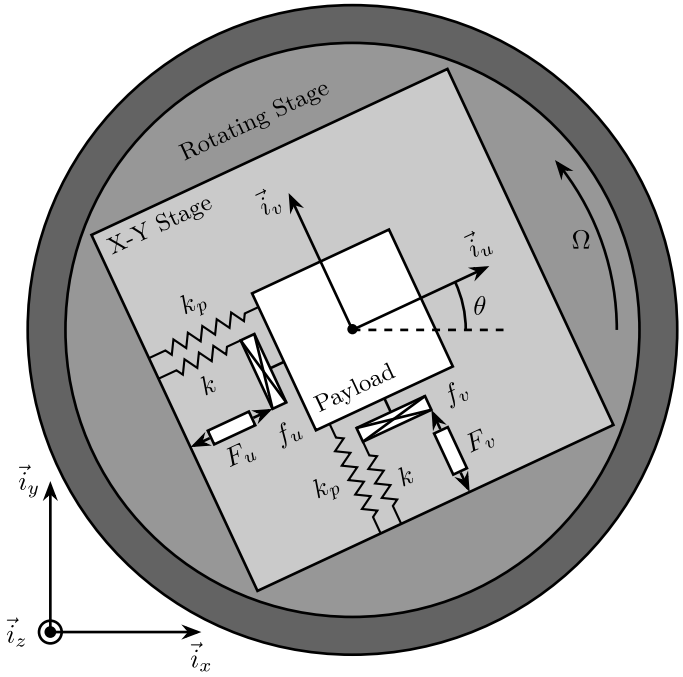

Figure 11: System with added springs k_p in parallel with the actuators

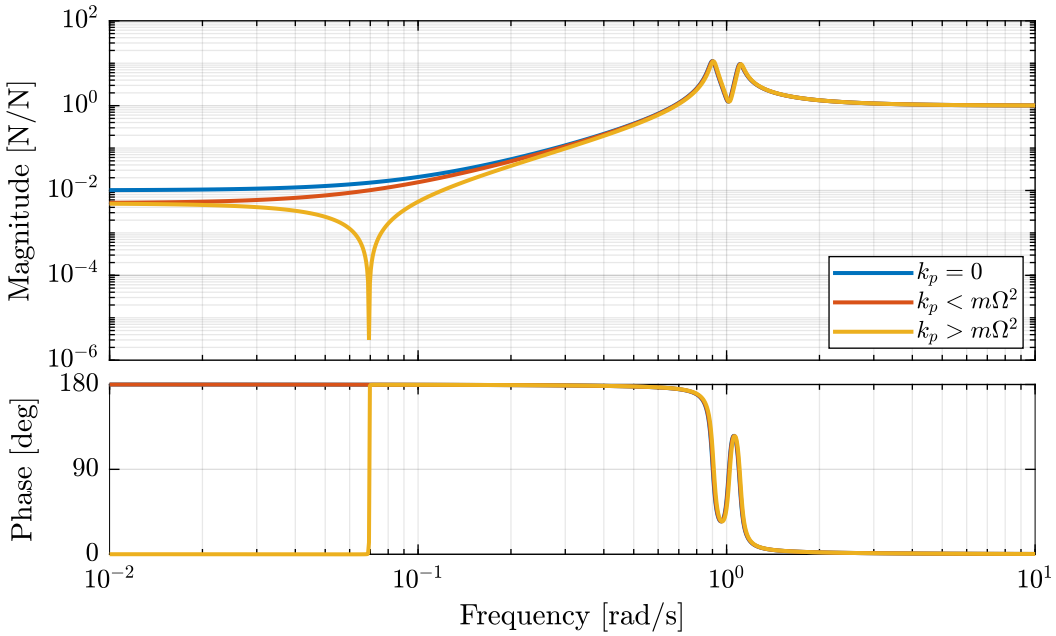

Figure 12: Bode Plot of f_u/F_u without any parallel stiffness, with a parallel stiffness $k_p < m\Omega^2$ and with $k_p > m\Omega^2$

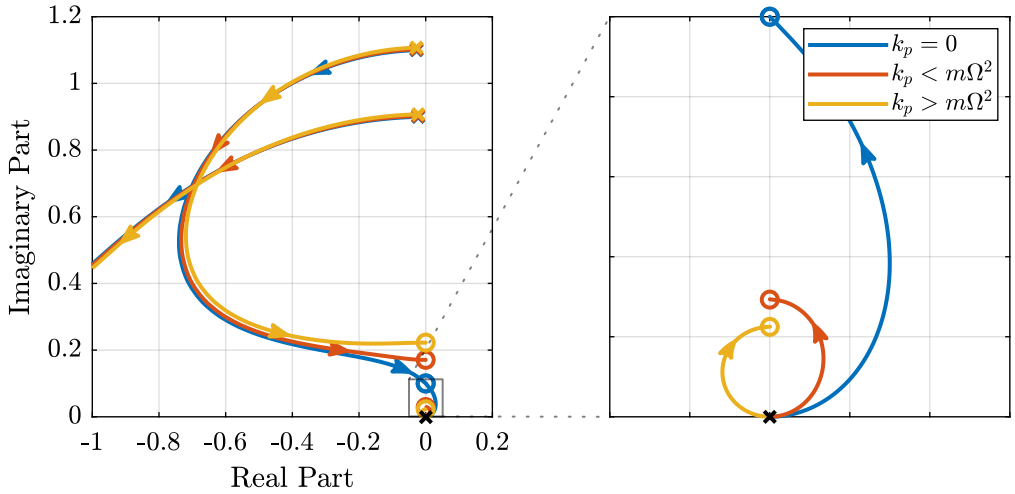

Figure 13: Root Locus for IFF without any parallel stiffness, with a parallel stiffness $k_p < m\Omega^2$ and with $k_p > m\Omega^2$

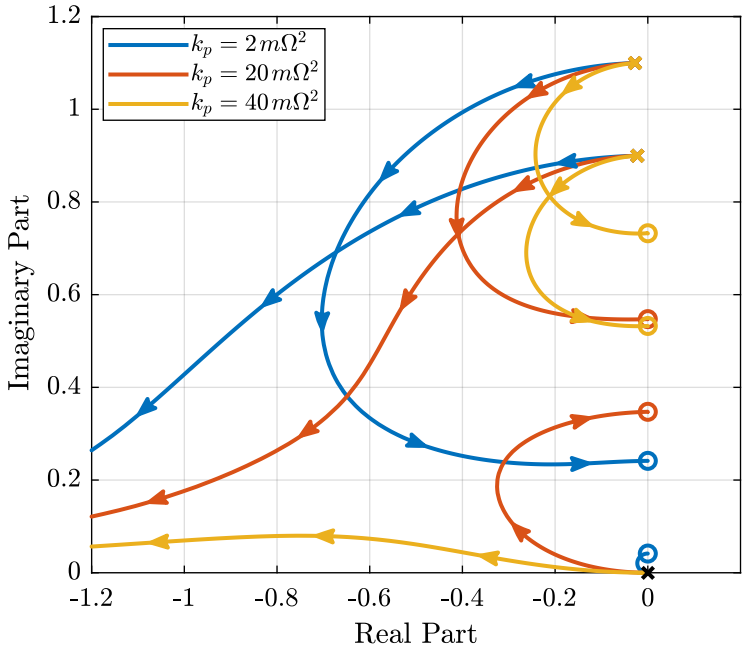

Figure 14: Root Locus for IFF for several parallel spring stiffnesses k_p

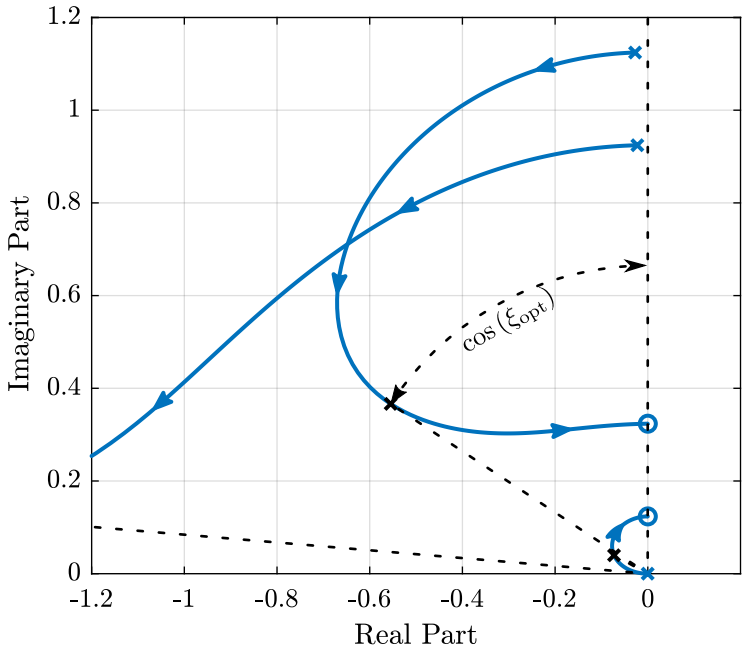

Figure 15: Root Locus for IFF with $k_p = 5m\Omega^2$. The poles of the system using the gain that yields the maximum damping ratio are shown by black crosses

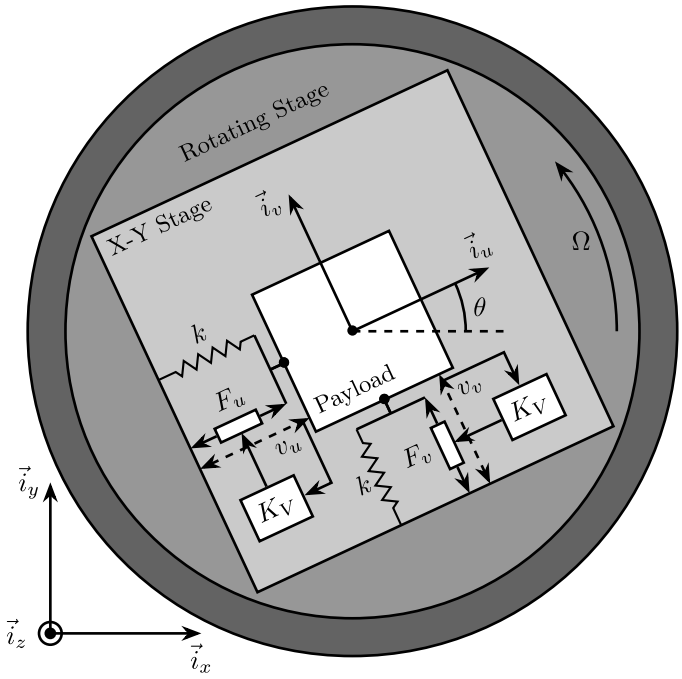

Figure 16: System with relative velocity sensors and with decentralized controllers K_V

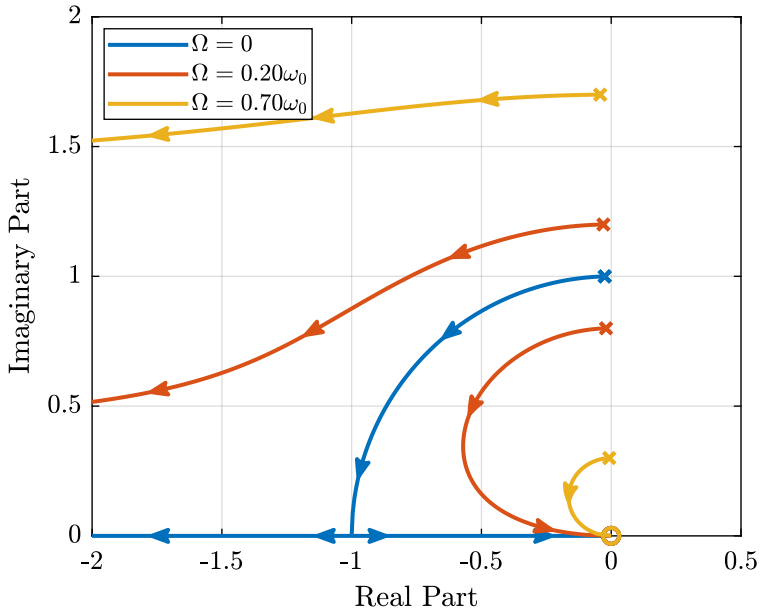

Figure 17: Root Locus for Decentralized Direct Velocity Feedback for several rotational speeds Ω

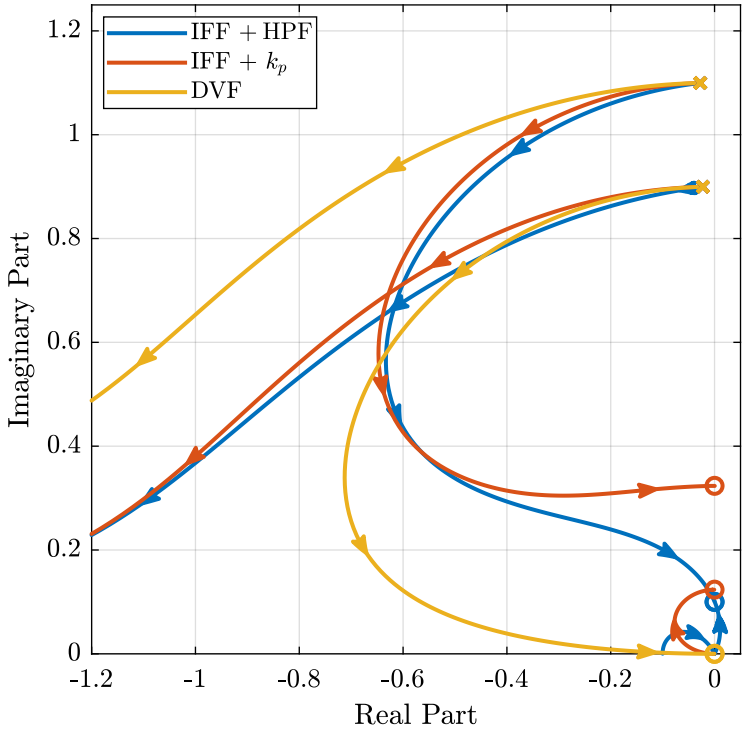

Figure 18: Root Locus for the three proposed decentralized active damping techniques: IFF with HFP, IFF with parallel springs, and relative DVF

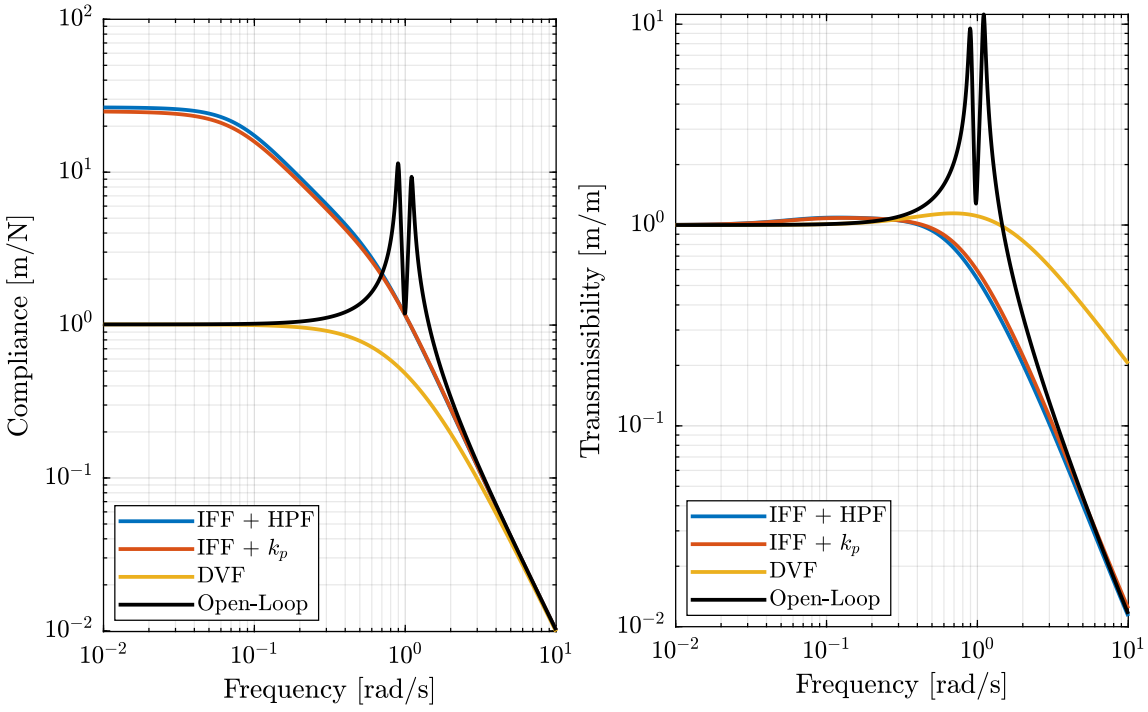

(a) Transmissibility

(b) Compliance

Figure 19: Comparison of the three proposed Active Damping Techniques

[1] T. Dehaeze, "Active damping of rotating positioning platforms," Source Code on Zonodo, 07 2020. [Online]. Available: https://doi.org/10.5281/zenodo.3894342